DISPERSION, ACTIVATION, AND DESTRUCTION OF AIRBORNE BIOLOGICAL THREATS: LABORATORY STUDIES OF THE INTERACTION OF SPORE-LADEN AEROSOLS WITH SHOCK/BLAST WAVES,

Petros Lappas, A. Daniel McCartt, Christopher Strand, Sean D. Gates,
David F. Davidson, Jay B. Jeffries, and Ronald K. Hanson
Mechanical Engineering Department, Stanford University, Stanford, CA, 94305-3032

Lydia-Marie Joubert
Cell Sciences Imaging Facility, Stanford University, Stanford, CA, 94305

Leslie A. Hokama and Kristien E. Mortelmans
Microbiology Department, SRI International, Menlo Park CA, 94025

ABSTRACT

A laboratory investigation of the interaction of shock waves with aerosols of bacterial spores (*Bacillus globigii (*BG*)* as a simulant of *B. anthracis*) is reported. Aerosols of BG are introduced in the test region of a gas-driven shock tube where they are subjected to shock waves of controlled strength. *In situ* laser diagnostics are used for time-resolved monitors of the scattering from the aerosols, gas temperature, and the dipicolinic acid (DPA) produced by spore rupture. These time-resolved measurements are complemented by *ex situ* analysis of collected samples of shock-treated spores, and the collection efficiency is calibrated by spore-sized SiO_2 counting beads as measured with flow cytometry. Viability of shock-treated spores is assessed by standard plating techniques. Post-shock spore morphology is assessed by scanning electron microscopy. Attenuation of ultraviolet light at 266 nm is found to provide a real-time *in situ* monitor of shock-induced spore rupture.

INTRODUCTION

Development of concepts for the cleanup and/or protection from airborne threats requires an understanding of the interactions of shock/blast waves with hazardous bio-aerosols. A variety of threats including toxic agents (e.g., incapacitating and lethal chemicals) and biological agents (e.g., incapacitating and lethal bacteria in spore and/or vegetative form, and viruses) can be delivered as airborne aerosols. Exposure of these aerosols with shock/blast waves has the potential to remediate or exacerbate the threat to security. The fate of hazardous aerosols after the passage of shock waves depends on many complex interactions, which have the potential to promote or eliminate the threat. For example, the threat could be magnified if liquid droplets were accelerated and spread over a wider region, where the acceleration will break up large droplets as the surface tension cannot support the aerodynamic forces. The threat could be further enhanced if the liquid water evaporates from the aerosol in the increased gas temperature behind the shock leaving a dry spore aerosol with a very long settling time. Conversely, the threat could be reduced if the increased temperature behind the shock wave produces thermo-chemical destruction. For bacterial spore aerosols, the post-shock heating could also increase the internal pressure inside the spore and mechanically fracture the spore membrane.

The Stanford aerosol shock tube (AST) facility provides a laboratory environment to expose aerosols containing bacterial spores to shock waves of controlled strength with real-time *in situ* laser monitoring and sampling of the shock-treated spores for *ex situ* diagnostics. Note that these shock waves correspond to blast waves in the atmosphere. Wavelength-multiplexed laser-scattering/absorption sensors developed previously [1] for the study of fuel chemistry provide measurements of the aerosol distribution, volume loading, and gas temperature as a function of time after the passage of a shock wave of controlled strength. For the study of bio-aerosols, these in situ diagnostics are augmented with three ex situ analyses of shock-treated samples. This suite of diagnostics tools and the Stanford AST facility enable the current program of experiments to investigate the interactions of shock waves with bio-aerosols, including:

(1) Development of new laboratory protocols for the study of shock waves with bacterial spores
(2) Shock-driven dispersion of aerosols.
(3) Shock-driven break up of large aerosol droplets into smaller (potentially more or less hazardous) aerosols.
(4) Shock-driven break up of solvent aerosols with imbedded surrogate bio-agents.
(5) Thermal evaporation of aerosols leading to gas-phase compounds and subsequent chemical reactions in the shock-heated air.
(6) Thermo-chemical destruction (or activation) of bio-hazards in aerosols through shock wave heating.
(7) Thermo-mechanical destruction (or activation) of bio-hazards in aerosols through shock wave acceleration and stress effects.

For the studies reported here, aqueous suspensions of *Bacillus globigii (*BG*)* were used as a simulants of *B. anthracis (BA)* spores. The strain (ATCC#9372) also referred to as *Bacillus subtilis* var. *niger* (American Type Culture Collection, Manassas, VA) was cultivated and spores havested. An aqueous suspension of BG spores was nebulized to produce a spore-laden water aerosol. The liquid water aerosol quickly evaporated as the aerosol was loaded into the shock tube. The dry BG spores were subjected to a shock wave of controlled strength while being monitored with three *in situ* laser extinction diagnostics Finally, the shock-treated spores were then collected for *ex situ* analysis. The sample collection efficiency was determined by flow cytometer analysis of samples collected before and after the shock treatment combined with the addition of 1μm diameter SiO_2 counting beads to the spore suspension used to produce the aerosol. In the work reported below, we find that the attenuation of ultraviolet (UV) laser light provided a real-time monitor of the products of spore rupture behind strong shocks. The fraction of the laser intensity attenuated was consistent with the amount of dipicolinic acid (DPA) available for release from the shock-exposed spores and our measurement of the absorption cross section for gas phase DPA. *Ex situ* examination of the collected spores using flow cytometry and scanning electron microscopy (SEM) indicates the spore morphology was predominantly intact following weaker shocks, yet standard plating techniques showed these shock-damaged spores were not viable.

AEROSOL SHOCK TUBE FACILITY

The Stanford aerosol shock tube consists of a driver section and a driven section separated with a diaphragm. The driven section can be divided with a sliding gate valve into two regions, an upstream section and a test section near the endwall. As illustrated in Fig. 1, the upstream

section is filled with bath gas and the test section filled with a mixture of bath gas and aerosol produced by a pneumatic nebulizer from an aqueous spore suspension. After the two driven sections are loaded, the endwall poppet valves are closed, the gate valve is opened, the driver section pressurized and the diaphragm bursts launching a planar shock which propogates into the driven section. The time evolution of the gas temperature and pressure observed at the laser diagnostic port near the endwall is illustrated in Fig. 2. When the incident shock arrives at t=0, the pre-shock (T_1, P_1) gas/aerosol mixture is abruptly heated and compressed (to T_2, P_2); when the shock wave reflected by the endwall arrives a second time at the measurement port, the gas is further heated and compressed (to T_5, P_5).

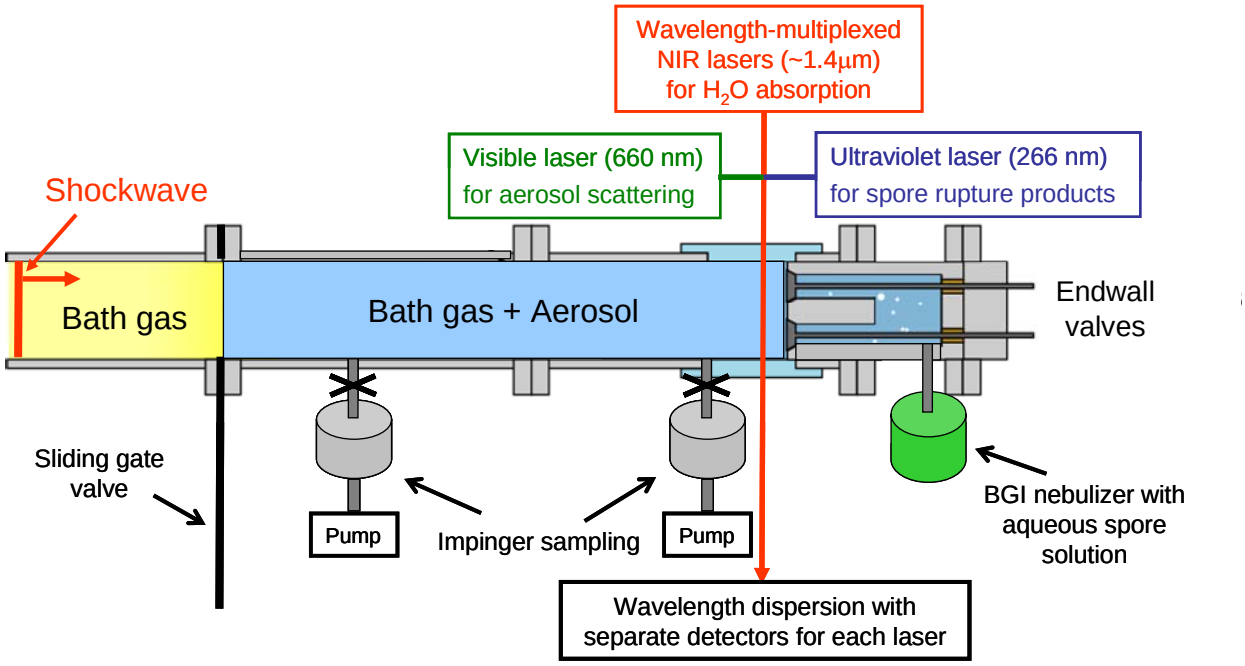

Fig. 1. Schematic of the driven section of the Stanford AST facility configured for shock-heating spore-laden aerosol. A gate valve can be closed to isolate the test region of the driven section near the endwall. When the gate valve is closed and the endwall valves open, aerosol laden bath gas produced by the gas dynamic nebulizer is loaded into the test section. The endwall valves are then closed, and the sliding gate valve opened before a shockwave is launched (as illustrated). Three *in situ* laser diagnostics monitor the shock-heated gas/aerosol, while pre- and post-shock samples are taken with gas dynamic impingers for *ex situ* analysis.

IN SITU DIAGNOSTICS

As illustrated in Fig. 1, the Stanford AST has three *in situ* laser monitoring diagnostics: visible for aerosol scattering, near-infrared (NIR) for H_2O absorption, and UV for aerosol scattering and absorption by the products of spore rupture. The laser beams from these three diagnostics are combined onto a common optical path, directed across the AST 5 cm from the endwall, collected and dispersed in wavelength onto separate detectors for each laser.

The visible laser extinction provides a monitor of the number density of dry spores, using the extinction cross section for BG spores taken from the literature.[2] For SiO_2 beads, the scattering cross section is calculated from the known SiO_2 bead diameter and index of refraction.

Water vapor is present in the bath gas from evaporation of the liquid water aerosols produced by the nebulizer. Two wavelength-multiplexed NIR lasers monitor absorption on water vapor absorption features near 1343.3 and 1391.7 nm, as illustrated in the two upper panels of Fig. 3. The lineshape curves monitor the absorbance versus laser wavelength and the stick figures mark the H_2O transitions that contribute to the measured signal. The internal energies of these two absorption features are different, and the ratio of the absorbance provides the gas temperature as shown in the lower panel of Fig. 3. Once the temperature is known, either of the laser measurements provides the H_2O concentration (providing a monitor of the amount of spore suspension loaded into the AST). Rapid scanning of the lasers provides 20μs time resolution, enabling fast, accurate measurements after the reflected shock wave arrives.

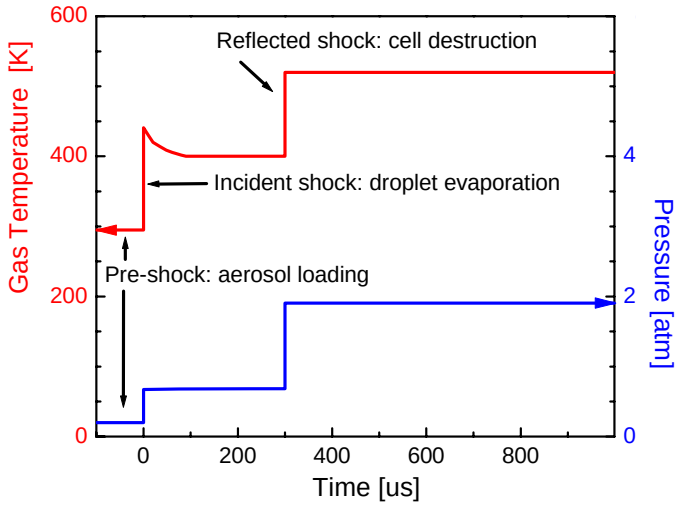

Fig. 2. Example of the time evolution of shock-heating of gas observed at the laser diagnostics port of Fig. 1. The graph illustrates a Mach=1.75 shock passing the measurement port, producing a rise of ~150 K temperature (top trace & left axis) and 3x pressure (bottom trace & right axis). The post-incident shock temperature then cools ~50K from the evaporation of the liquid-water aerosol. The reflected shock produces another ~200K temperature rise and 3x pressure increase. Such a shock is produced by a driver gas pressure ~9 atm with a 0.2 atm driven gas pressure.

In the results section below, we discover that when BG spores are exposed to strong shock waves, the spore walls rupture, and the products attenuate the transmitted UV laser light in the shock tube. It has long been known that DPA is present in spores [3], where it accounts for 5-15% of the dry mass [4]. In the commonly used test strain *B. subtilis*, the release of 2×10^8 molecules of DPA per spore was reported [5]. Processes involving the structural rupture of spores such as autoclaving, chemical lysis, and germination are known to result in the release of DPA into the spore's environment [6]. The appearance of DPA in the test gas could serve to measure the extent of spore rupture. We postulate that absorption by DPA contained in the spore

is the source of the attenuation of the UV laser (or subsequent products of thermal decomposition of DPA). A large UV absorption cross section has been reported in the literature [7]; however, these data are for DPA in aqueous solution. Spore rupture behind the shock waves will produce gas-phase products or aqueous aerosols where the water will quickly evaporate. Therefore, experiments were conducted to measure the gas-phase DPA absorption cross section.

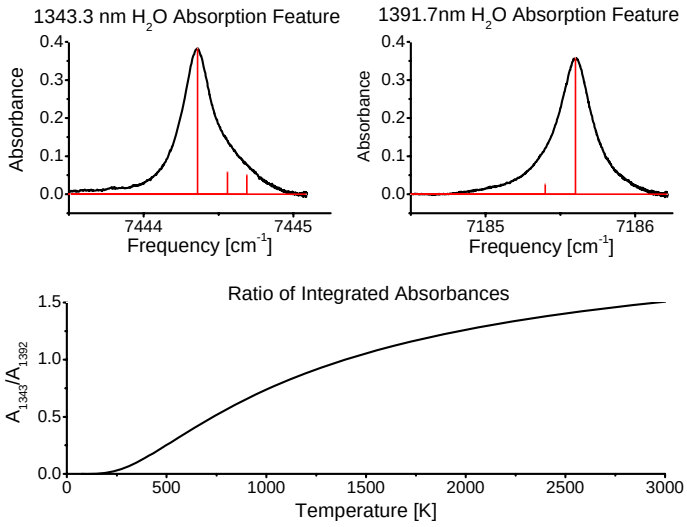

Fig. 3. Upper two panels illustrate absorption versus wavelength tuning of two water vapor absorption features (near 1343.3 and 1391.7 nm). Measured post-reflected shock T_5=1397K, P_5=5.97atm. The vertical bars illustrate the relative contribution of the multiple individual transitions in each of these well-resolved features. The wavelength is rapidly scanned providing absorption measurements on both features every 20 μs. The lower panel shows ratio of the integrated absorption of the two features is a function of gas temperature.

ABSORPTION MEASUREMENTS OF DPA

The AST was used for measurements of the UV absorption of DPA (or thermal decomposition products of DPA) at the high temperatures where we observe spore rupture. An aqueous aerosol containing DPA was produced by an ultrasonic nebulizer using an aqueous solution of synthetic DPA (Sigma-Aldrich), and this DPA-laden fog was entrained in a water-vapor-saturated argon bath and loaded into the AST through the endwall poppet valves.

All three of the *in situ* laser diagnostics are used for these AST experiments, and typical data are illustrated in Fig. 4. Before the arrival of the incident shock both the 266 nm and the 670 nm lasers are scattered by the water aerosol at the loading pressure and temperature (P_1, T_1). When the shock wave arrives, the transmitted beam is steered by the density gradient producing a "Schlieren spike" in the laser extinction data. Behind the incident-shock the aerosol/gas mixture is compressed and heated (to P_2, T_2), and the scattering extinction increases for both 266 and 670 nm. At the higher temperature behind the incident shock wave (T_2), the bath gas is no longer saturated in water vapor, and the aerosol begins to evaporate, with the decrease of extinction reflecting the rate of evaporation.

When the reflected shock arrives the mixture is heated and compressed yet again (to P_5, T_5), and any remaining water droplets quickly evaporate. The 670 nm scattering data after the reflected shock has no attenuation (zero extinction). Although the two NIR colors, ~1343.3 and ~1391.7 nm, of the water vapor diagnostic also show the same scattering before the aerosol evaporates, these data are not shown in the figure for clarity. However in the region after the reflected shock where all the liquid-water aerosol has evaporated, these two laser beams also are attenuated by the water-vapor absorption when their wavelength is tuned through the water vapor absorption feature. This extinction is illustrated in Fig. 4. The ratio of the two NIR absorption signals is a function of gas temperature and the value determined agrees well with T_5 determined from the measured shock speed [8].

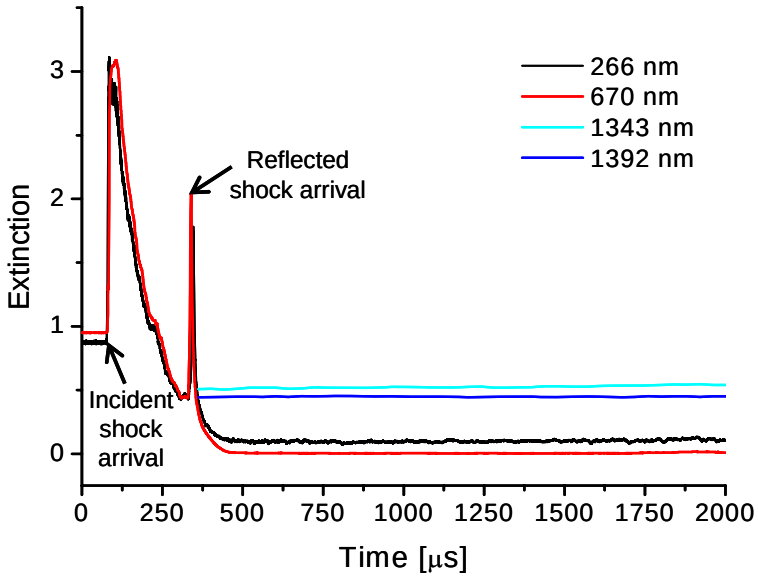

Fig. 4. Extinction data for 266, 670, 1343.3, and 1391.7 nm lasers as a function of time following shock heating of an aqueous aerosol from DPA/water solution (2g/l) (P_1=0.232 atm, P_2=1.6 atm, P_5=6.6 atm, T_1=295 K, T_5=900 K) in the Stanford AST. The difference between the 266 nm and 670 nm data after the reflected shock arrives is a measure of gas phase absorption of DPA at 900 K.

After the arrival of the reflected shock, the 266 nm UV light shows the extinction due to the absorption of DPA, while the visible 670 nm light is not attenuated (i.e. goes to zero extinction) after the liquid aerosol is fully evaporated. Assuming all of the post-reflected-shock extinction is due to DPA absorption, this experiment yields an absorption cross section of 2.1×10^{-17} [cm^2/molecule] at 900 K. There is some potential that the DPA thermally decomposes at these temperatures [9]. However, the data in Fig. 4 illustrate that if DPA does significantly thermally decompose in the millisecond test time, the decomposition products efficiently absorb 266 nm laser light providing a marker of DPA, and hence a monitor of DPA production from spore rupture at similar temperatures. In the discussion below of shock-heated BG spore experiments, we will find this 266 nm extinction diagnostic provides a real-time monitor of spore rupture.

SHOCK HEATING OF BG SPORE AEROSOL

The destruction of BG spores by shock waves was investigated using two different experimental protocols: (1) quantitative viability studies of shock heated spores using *ex situ* diagnostics and (2) real-time *in situ* monitoring of spore rupture products using 266 nm ultraviolet absorption. For these experiments, aqueous suspensions of unclumped BG were prepared with a high density of BG (~ $(10)^{10}$ viable CFU/ml). This suspension was diluted (10^6-10^8 CFU/ml) and mixed with 1μm diameter SiO_2 counting beads. The spore/bead aqueous suspension was loaded (3-5 ml) into the reservoir of a commercial, pneumatic nebulizer (Collison type, BGI Inc.) [10]. Aerosols of BG spores have been reported using this nebulizer without loss of viability [11]. Spore samples were collected as a function of residence time in the nebulizer, and even after ~10 minutes, plating of these samples showed no discernible change in viability.

For quantitative viability studies, samples of the shock-treated spores were examined with three *ex situ* diagnostics: (1) plating for viability, (2) flow cytometry for calibration of the collection efficiency, identification of damage to the spore wall, and complete destruction of the spore, and (3) SEM for morphology and identification of structural damage to the spore. Samples were collected using a gas dynamic impinger (Ace Glass Inc.) before and after shock heating. Two impingers were attached to the test region of the AST as illustrated in Fig. 1. A small sample of the bath gas/aerosol was collected with the upstream impinger after the test region of the shock tube was filled, just prior to opening the sliding gate valve. The downstream impinger was used to collect the shock-treated spores at the conclusion of the experiment. In the impinger, exhaust from the AST was choked by a converging nozzle and directed onto a pool of water (5-10 ml), so that particulate in the flow impacts the water, where it was captured, while the gas flow was pumped away.

The viability of the collected sample was determined by standard plating techniques, i.e., diluting and plating on nutrient agar (NA) plates. After overnight incubation at 37 C the colonies on the plates were counted. The plates were then kept at room temperature for an additional 48 hours to insure the colony count had stabilized. The viability of an untreated control spore suspension was determined in parallel with each experiment.

The BG spores and the SiO_2 counting beads in the collected samples were counted by flow cytometry (BD BioSciences model FACScan). The SiO_2 counting beads were chosen to have approximately the same size as the BG spores, to insure similar uptake into the aerosol and dispersion in the shock tube. Despite the similar size, the difference in morphology and index of refraction allows them to be readily distinguished by the ratio of forward to side scattering of light in the flow cytometer, as illustrated in Fig. 5. This measurement provides the number of SiO_2 bead and intact spores for every pre-shock and post-shock sample. The ratio of beads to spores in all of the pre-shock samples was identical to the ratio of beads to spores in the nebulizer reservoir. Thus, measurement of the SiO_2 beads provides a measurement of the collection efficiency of the post-shock samples.

Dry BG aerosol was subjected to shock waves in argon and argon/oxygen mixtures with post reflected shock temperatures ranging from 560-1100K. For all of these experiments >99% of the pre-shock viable spores were not viable in the post-shock sample. The test time in these experiments was less than 10 ms, and thus even this brief exposure to high temperatures behind shock waves was sufficient to significantly suppress the viability of dry BG spores.

Flow cytometry of the post-shock samples found two distinctly different outcomes. For strong shocks with T_5~900 K, we find >99.9% of the spores were destroyed, while for weaker

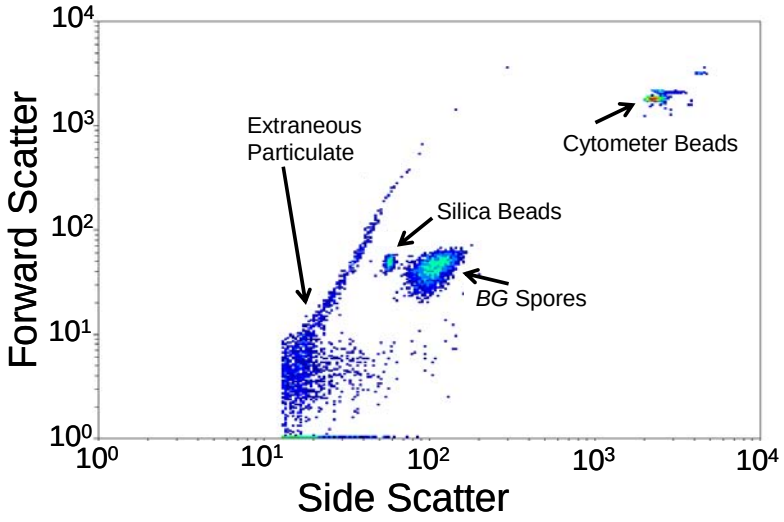

Fig. 5. Typical flow cytometer analysis of pre-shock samples.

shocks T_5~600K, we found ~80% of the spores could be identified in the flow cytometer. These results suggest that the spore wall was damaged by the shock wave, and one would expect the organelles to have been exposed to the environment. This is consistent with the flow cytometry fluorescence results from collected samples stained with propidium iodide (PI) dye (Molecular Probes, Invitrogen, CA). This dye is activated when it binds to nucleic acids, but is excluded by viable cells, as it can only penetrate compromised cell membranes of dying or dead cells [12]. The fluorescence measured by the flow cytometer for the post-shock (T_5~600K) samples stained with PI was approximately five times more intense than dye-stained pre-shock samples.

This hypothesis of organelles leaking from shock-treated spores was further confirmed by SEM analysis of the post-shock samples for the T_5~600 K experiments. Portions (50 µl) of the impinger samples were filtered (0.22µm cellulose, Millipore, MA), air-dried, and mounted on double-sided carbon tape on aluminum stubs (Electron Microscopy Sciences, PA). Portions (1ml) of some of the samples were centrifuged (5,000 rpm for 5min) to concentrate the collected material, and 50µl sub-samples from the tip of the Eppendorff tube were air-dried on carbon tape attached to aluminum stubs. All stubs were thereafter sputter-coated (100 Å layer) with gold-palladium in a Denton Vacuum Desk II unit, and visualized with secondary electron detection with a Hitachi S-3400N VP-SEM, operated under high vacuum at 10 and 15kV at a working distance of 8-9mm. Images (2560x1920 pixels) were captured with a CCD camera.

The four SEM images in Fig. 6 illustrate the results (note only panel D shows a centrifuged sample). Panel A shows a typical pre-shock sample. The round SiO_2 beads are quite distinct from the BG spores which are primarily unclumped single spores. Panel B illustrates one shriveled and clearly damaged spore along with two SiO_2 beads after shock-heating in argon/O_2 with T_5=561 K; note the background mesh is the filter material. The image in panel C contains beads, damaged spore coat, and organelles, clearly illustrating the severe damage to the cell walls followed by leaking of the organelles into the environment. Panel D shows a sample centrifuged to concentrate the spore material; note how the sticky organelles tend to clump all of the collected material into one large aggregate of organelle material.

The complete destruction of countable spores in the flow cytometer for the samples treated to high temperature shocks (T_5~900K) led us to investigate the potential of using UV extinction to monitor spore destruction in real time. For these experiments, the BG density was increased

in the BGI nebulizer to 10^{10} CFU/ml, and to avoid the UV scattering from the SiO_2 beads, they were not added to the nebulizer suspension.

When dry BG aerosol is exposed to strong shocks, the products of spore rupture can be observed with *in situ* UV laser transmission. The results of time-resolved extinction of the visible and UV diagnostics during such an experiment in the AST is illustrated in Fig. 7, where a dry BG aerosol is shock heated in argon bath gas (P_1= 0.549 atm, P_2=3.35 atm, P_5=12.05 atm, T_1=296 K, T_2=684K, T_5=1162 K). Before the arrival of the incident shock wave, both laser beams are attenuated by scattering/absorption from the BG spores. When a shock wave arrives, the beam steering in the density gradient produces a "Schlieren spike" in the laser attenuation data. Behind the incident shock wave, the test gas mixture of BG aerosol and argon is heated (T_2) and compressed (P_2) producing an increase in the laser extinction signals. When the reflected shock arrives, the extinction of both beams increases again to reflect the increase in temperature (T_5) and density (P_5). However, at the high temperature behind this strong shock wave (1162 K), the BG spores quickly rupture and the scattering attenuation of the visible laser drops to near zero in ~25 μs. We believe this is the first observation of time-resolved spore rupture in high temperature gases, and further work to validate this preliminary result and quantify rate of rupture vs temperature is planned.

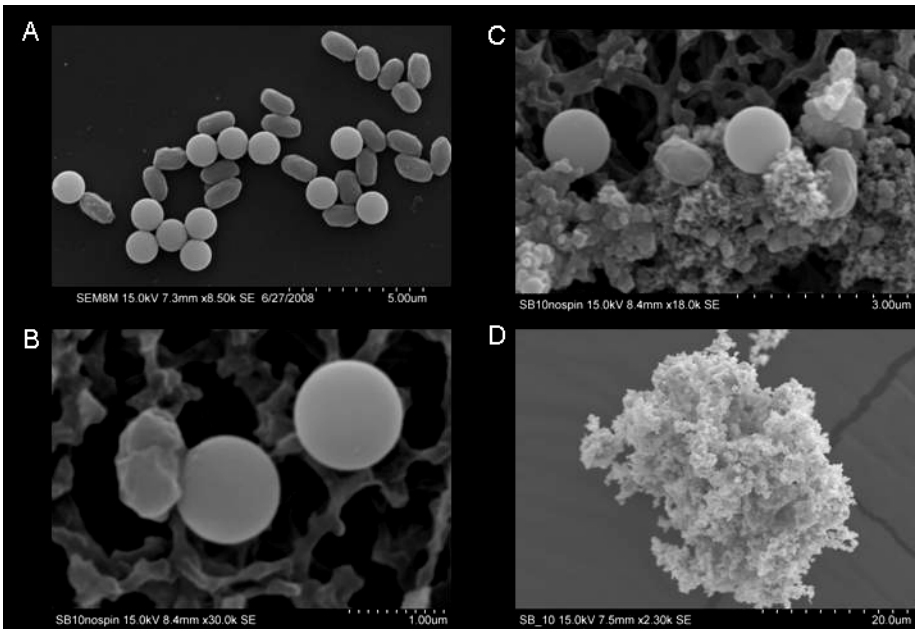

Fig. 6. SEM images of spores and SiO_2 beads collected from the AST; note the scale bar in the lower right corner of each image corresponds to 5μm in panel A, 1μm B, 3μm is C and 20μm in D. Panel A illustrates the morphology of the BG spores and SiO_2 beads collected pre-shock. Panels B-D illustrate material collected after shock treatment (T_5=561K) of dry spore/bead aerosol in an argon/oxygen mixture. Panel B shows the damage to individual spore walls by the shock. Panel C shows the large amount of organelle material present along with the fractured spore coats. Panel D shows how the organelle material promotes clumping when the collected sample is centrifuged.

The UV extinction in Fig. 7 also decays in the first 25 μs after the arrival of the reflected shock wave, but does not drop to near zero like the visible diagnostic. We surmise the relatively constant extinction after the initial decay following the reflected shock heating is due to absorption of the products of spore rupture. If we assume that all of this 266 nm extinction is due to absorption of DPA, we get a DPA mass consistent with the literature. We estimate the spore density behind the reflected shock wave to be ~1x10^5 spores/cm^3 using the measured visible scattering before the incident shock with the visible scattering cross section for BG spores reported by Walts et al.[2] and the known compression of the well-characterized shock waves [8]. Using our measured absorption cross section for high-temperature DPA (or potentially DPA decomposition products), the absorption of the 266nm laser after the reflected shock wave indicates a release of ~5±2 x10^8 DPA molecules per BG spore for the data in Fig. 7. Assuming 100% spore rupture to 100% DPA product this corresponds to a DPA release of 15±6% of the BG dry mass, which is consistent with the reported mass fraction of DPA in BG spores.[5]

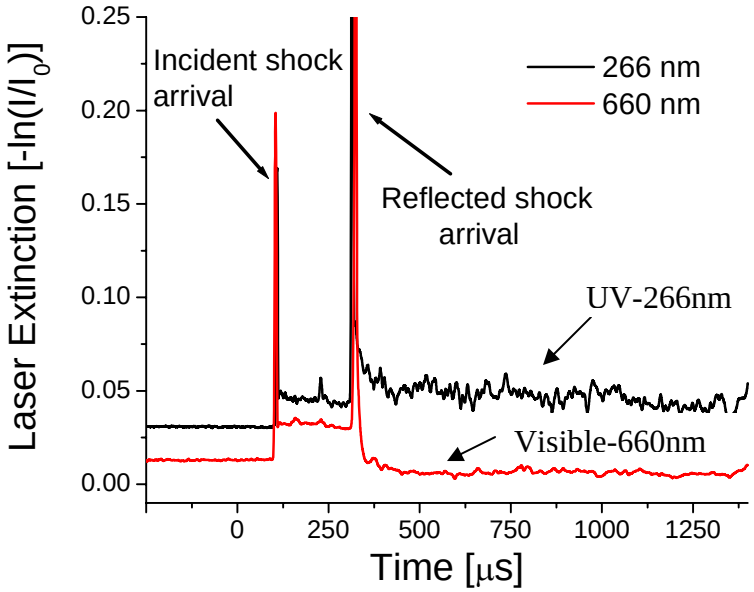

Fig. 7. Time-resolved laser extinction for 266 and 660 nm (P_1= 0.549 atm, P_2=3.35 atm, P_5=12.05 atm, T_1=296 K, T_2=684K, T_5=1162 K). Before the incident shock wave arrives, both lasers are attenuated by the extinction by the dry BG spores. The spore-laden bath gas is heated and compressed by the incident shock and then again by the reflected shock. After the reflected shock, the break up of the spores is evidenced by the drop in the Mie scattering of the 660 nm light. The continued extinction of the 266 nm light reflects gas phase absorption by the products of the spore rupture.

CONCLUSIONS

A new laboratory paradigm for the study of interactions of bacterial spores with shock/blast waves of controlled strength is demonstrated. This experimental method allows for a variety of *in situ* and *ex situ* diagnostics. The *in situ* diagnostic suite used consisted of ultraviolet, visible, and near-infrared laser extinction measurements, while the *ex situ* analysis includes plating, flow cytometry and scanning electron microscopy. The *in situ* laser diagnostics provide time-resolved

measurements of the spore aerosol, gas temperature, and the release of products from spore rupture. The *ex situ* plating of the collected samples provides spore viability, the flow cytometry data yields quantitative collection efficiency even when the spores are destroyed, and the SEM images provide interpretation of the outcome of the shock heating.

Dry aerosols of BG spores mixed with SiO_2 counting beads are produced and loaded into a gas-driven shock tube. Samples of the aerosol are collected before and after shock treatment and the collection efficiency determined by flow cytometry counting of the SiO_2 beads, which are unharmed by the temperature and pressure increase behind the shock waves. The viability of BG spores is reduced more than two orders of magnitude after treatment with shock waves with T5 ranging from 550-1200 K. The test time in these experiments is less than 10 ms, and thus even this brief exposure to high temperatures behind shock waves is sufficient to significantly reduce the viability of dry BG spores. Analysis of the collected samples by flow cytometry shows two distinct outcomes: strong shocks (T_5~900K) destroy the spore morphology while weaker shocks (T_5~600K) kill nearly all the spores, but leave ~80% of the spore walls intact to be counted by flow cytometry. This interpretation was consistent with SEM analysis of the shock-heated samples. UV absorption by the products of spore rupture was demonstrated and provides the potential for a real time monitor of spore destruction.

ACKNOWLEDGEMENTS

The authors acknowledge the support of the Army Research Office and the Defense Threat Reduction Agency. Christopher Hutson (SRI International) is acknowledged for his work in spore preparation and viability measurements.

REFERENCES

1. D.F. Davidson, D.R. Haylett, R.K. Hanson, “Development of an aerosol shock tube for kinetic studies of low-vapor-pressure fuels,” *Combustion and Flame* (2008) in press.
2. S.C. Walts, C. A. Mitchell, M.E. Thomas, D.D. Duncan, “Extinction cross-section measurements of *Bacillus globigii* aerosols,” *Johns Hopkins Applied Physics Laboratory Technical Digest* **25** (2004) 50-55.
3. J.F. Powell, “Isolation of dipicolinic acid (pyridine-2:6 dicarboxylic acid) from spores of *Bacillus megatherium*,” *Biochemical J.* **54** (1953) 210-211.
4. W. G. Murrell, “Chemical composition of spores and spore structures,” in *The Bacterial Spore*, G.W. Gould, A Hurst (Eds), Academic Press, New York, 1969, pp. 215-274.
5. A.A. Hindle, E.A.H. Hall, "Dipicolinic acid (DPA) assay revisited and appraised for spore detection," *Analyst* **124** (1999) 1599-1604.
6. P.M. Pellegrino, N.F. Fell, and J.B. Gillespie, "Enhanced spore detection using dipicolinate extraction techniques," *Analytica Chimica Acta* **455** (2002) 167-177.
7. R. Nudelman, B.V. Bronk, S. Efrima, “Fluorescence emission derived from dipicolinc acid, its sodium, and its calcium salts,” *Applied Spectroscopy* **54** (2000) 445-449.

8. A. G. Emanuel, “Shock waves in gases,” Chapter 3 Section 3.1 in *Handbook of Shock Waves: Volume 1, Theoretical, Experimental and Numerical Techniques*, G. Ben-Dor, O. Igra, T. Elperin (Eds) Academic Press, New York, 2001, pp. 185-262.

9. Tripathi, W.M. Maswadeh, A.P. Snyder, “Optimization of quartz tube pyrolysis atmospheric pressure ionization mass spectrometry for the generation of bacterial biomarkers,” *Rapid Commun. Mass Spectrometry* **15** (2001) 1672-1680.

10. K.R. May, “The Collison nebulizer: description, performance and application,” *Aerosol Science* **4** (1973) 235-243.

11. R.C. Stone, D.L. Johnson, “A note on the effect of nebulization time and pressure on the culturability of *Bacillus subtilis* and *Pseudomonas fluorescens*,” *Aerosol Science and Technology* **36** (2002) 536-539.

12. C.Y. Chen, G. Seguin-Swartz, “A rapid method for assaying the viability of fungal spores,” *Canadian J. Plant Pathology* **24** (2002) 230-232.